I&EC research
Industrial & Engineering Chemistry Research

Article

pubs.acs.org/IECR

Closed-Loop Compensation Method for Oscillations Caused by Control Valve Stiction

Jiandong Wang*

College of Engineering, Peking University, Beijing, China 100871

ABSTRACT: This paper proposes a closed-loop compensation method to remove oscillations caused by control valve stiction. With the control loop operating at the auto mode, the proposed method adds a short-time rectangular wave to the reference to introduce two movements for the control valve to arrive at a desired position. A systematic way to design the parameters of the short-time rectangular wave is developed. The proposed method is robust against modeling errors and measurement noises. The effectiveness of the proposed method is illustrated by laboratory and simulation examples.

1. INTRODUCTION

Industrial surveys[1−3] reported that about 20−30% of control loops in various process industries perform poorly due to control valve nonlinearities. One typical abnormal phenomenon is the oscillation of signals in a closed-control loop caused by control valve stiction. Hence, it is practically important to detect the presence of stiction and to quantify the stiction severity. Once the stiction has been detected and quantified, the control valve can be scheduled for maintenance or replacement. However, it is often desirable to keep using the sticky control valve, and to compensate the negative effects of stiction by temporarily removing oscillations.

In the last a few years, the detection and quantification of control valve stiction have been very active research topics.[4] However, there are relatively fewer studies on the compensation of control valve stiction. Gerry and Ruel[5] listed four suggestions for combating stiction online, e.g., removing integral action of the proportional−integral (PI) controller; doing so usually leads to large steady-state control errors and works only for nonintegrating processes.[6] Hägglund[7,8] presented a so-called knocker method to add short pulses to controller outputs in order to keep control valves moving. Srinivasan and Rengaswamy[9] integrated a stiction estimation procedure with the selection of parameters for the knocker method. Ivan and Lakshminarayanan[10] revised the knocker method by replacing the short pulses with constant reinforcements added to controller outputs. Both the knocker method[7,8] and the constant reinforcement method[10] reduce the variation of process outputs at the cost of aggressive valve movements that may wear valves quickly. To avoid the aggressive valve movements, Srinivasan and Rengaswamy[11] proposed a two-move method and an optimization-based method for stiction compensation. The two-move method adds two compensation movements to the controller output in order to make the control valve eventually arrive at a desired steady-state position. Cuadros et al.[12] improved the two-move method by introducing more movements to controller outputs. Later, Cuadros et al.[13] proposed another model-free compensation approach by monitoring the control errors after a knocker is introduced: if the knocker happens to move the valve to a desired position so that the control error is small for a certain period of time, then the controller is disabled. Mohammad and Huang[14] eliminated oscillations caused by control valve stiction or reduced the magnitude and frequency of oscillations by tuning controller parameters. There are also some methods to compensate the negative effects of valve friction for control tasks,[15,16] which are not aimed at temporarily removing oscillations, and thus are not applicable in this context.

This paper is inspired by the two-move method[11] and its improved versions.[12] However, these two-move methods have to switch to the open-loop control, which may not be allowed sometimes in practice owing to various operational requirements. By contrast, a closed-loop compensation method is proposed here, without switching to the open-loop control. The proposed method adds a short-time rectangular wave to the reference to achieve the same two valve movements as in the two-move methods. To achieve this, the parameters of the short-time rectangular wave are designed in a systematic manner: based on the stiction model with two parameters proposed by He et al.,[17] signals in different stages are analyzed, analytic functions and conditions to be satisfied by the design parameters are derived, and a procedure to obtain optimal design parameters is devised. The proposed method by design has a certain level of robustness against modeling errors and measurement noises; in addition, a deadband is introduced to ignore small control errors after compensation.

Among the existing compensation methods, the knocker method,[7,8] the constant reinforcement method,[10] the method proposed by Cuadros et al.[13] and that by Mohammad and Huang[14] keep the control loop operating at the auto mode; however, as stated earlier, the knocker method and the constant reinforcement method suffer from the drawback of introducing aggressive valve movements. Hence, only the method proposed by Cuadros et al.[13] and that by Mohammad and Huang[14] are compared here with the proposed method.

- The method proposed by Cuadros et al.[13] is based on a critical assumption: if the variations of the control error after using the knocker method are kept small for a certain time duration, then it implies that the valve position arrives at the position associated with a desired

Received: January 27, 2013
Revised: July 29, 2013
Accepted: August 1, 2013
Published: August 1, 2013

dx.doi.org/10.1021/ie400308z | *Ind. Eng. Chem. Res.* 2013, 52, 13006−13019

reference value. However, there is no guarantee for the assumption to be always hold. The reason is that the knocker method may achieve the small control errors by fast switching among several valve positions; once the compensation method proposed by Cuadros et al.[13] disables the PI controller, the valve may stay a position quite far away from the desired one, resulting in a large control error (see example 3 in section 4 for an illustration).

- The method proposed by by Mohammad and Huang[14] does not consider where the control valve stays after removing the oscillations by tuning controller parameters. As a result, the control error could be quite large even if it is no longer oscillatory after compensation (see example 4 in section 4).

By contrast, the proposed method aims at making the control valve arrive at a desired position after compensation, so that the control error is small after compensation. Nevertheless, the method proposed by Cuadros et al.[13] and that by Mohammad and Huang[14] require less information than the proposed one and, thus, are easier to implement.

The rest of the paper is organized as follows. Section 2 describes the compensation problem. Section 3 presents the closed-loop compensation method. The effectiveness of the compensation method is illustrated through laboratory and numerical examples in section 4. Some concluding remarks are given at section 5.

2. PROBLEM DESCRIPTION

Consider a closed-control loop with a control valve depicted in Figure 1, where $r(t)$, $e(t)$, $m(t)$, $v(t)$, $y_m(t)$, and $w(t)$ are the

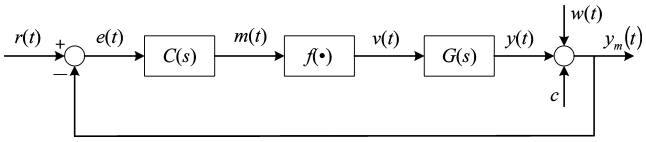

Figure 1. Diagram of a closed-control loop.

reference, control error, controller output, valve position, measured process output and process noise/disturbance, respectively. The process $G(s)$ is confined to be a linear time-invariant (LTI) process that is described as

$$G(s) = \frac{K\mathrm{e}^{-\theta_0 s}}{\Pi_{i=1}^{I}(\tau_{0,i}s + 1)} \tag{1}$$

Such a process can be approximated well by a first-order plus dead time (FOPDT) model[18]

$$G(s) = \frac{K_\mathrm{p}}{T_\mathrm{p}s + 1}\mathrm{e}^{-\theta s} \tag{2}$$

A proportional−integral (PI) controller $C(s)$ is used

$$C(s) = K_\mathrm{c}\left(1 + \frac{1}{T_i s}\right) \tag{3}$$

The controller is implemented at an industrial distributed control system (DCS) platform with the sampling period T_s. In Figure 1, c is a real-valued constant to take care of the static offset of $y_\mathrm{m}(t)$ so that the noise-free process output $y(t)$ is a deviation signal. The control objective is to let $y_\mathrm{m}(t)$ close to a desired reference value r_0.

The control valve, denoted by $f(\cdot)$ in Figure 1, is assumed to have the stiction problem. There are several data-driven stiction models in the literature,[4] among which the model with two parameters proposed by He et al.[17] is adopted here. The flowchart of the stiction model is presented in Figure 2. The parameters f_s and f_d in Figure 2 stand for the static and kinetic

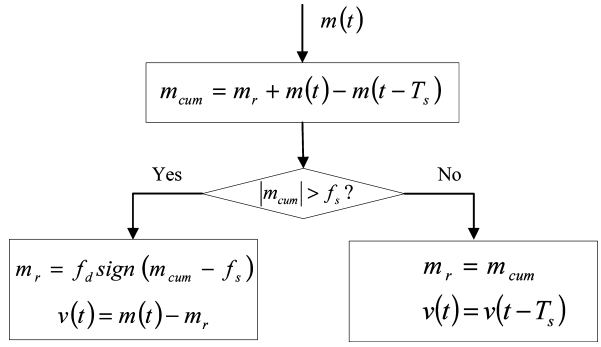

Figure 2. Flowchart of the stiction model proposed by He et al.[17] Adapted from Figure 2 of ref 17. Copyright 2007 American Chemical Society.

friction bands, respectively. The variable m_r is the residual force acting on the valve which has not materialized a valve movement, and the variable m_cum is a current cumulative force acting on the valve.

Even though the reference $r(t)$ takes a constant value r_0, the control valve stiction may lead to oscillations in the loop, affected by some nonzero initial condition and/or driven by process noise/disturbance $w(t)$. This phenomenon has been observed for many industrial control loops (see e.g., the international database [available online at http://www.ualberta.ca/~bhuang/book2.htm] associated with the book[4]), and can be theoretically shown via the describing function analysis. For instance, such an analysis has been performed for a particular data-driven stiction model.[6]

The compensation problem is to design a compensation method to temporarily remove the oscillations caused by the control valve stiction, based on the oscillatory data of $y_\mathrm{m}(t)$ and $m(t)$.

3. CLOSED-LOOP COMPENSATION METHOD

This section proposes a closed-loop compensation method that solves the compensation problem with the control loop operating in auto mode. To ease the presentation, the process noise/disturbance $w(t)$ is assumed to be absent for the time being.

3.1. Main Idea. If the control valve has no stiction, then the valve position $v(t)$ is able to arrive at a steady-state value, denoted as v_ss, to achieve zero control error. The value of v_ss is

$$v_\mathrm{ss} = \frac{r_0 - c}{K_\mathrm{p}} \tag{4}$$

where r_0 is the desired reference value, K_p is the process gain in eq 2, and c is the static offset of $y_\mathrm{m}(t)$ (see Figure 1). When the stiction is present, however, $v(t)$ cannot reach v_ss. Instead, $v(t)$ jumps around v_ss in a periodic manner, leading to oscillations in the loop.

When the oscillations occur, the characterization of the stiction model is demonstrated in Figure 3. When the valve moves, the relation between $m(t)$ and $v(t)$ is

$$v(t) = m(t) \pm f_\mathrm{d} \tag{5}$$

Here the summation (subtraction) sign is used if $m(t)$ is decreasing (increasing). Owing to the stiction, the control valve can only move along the increasing path l_a or the decreasing path l_d, e.g., the valve may only stay at the positions marked by filled-circles in Figure 3 when the oscillations occur.

dx.doi.org/10.1021/ie400308z | Ind. Eng. Chem. Res. 2013, 52, 13006−13019

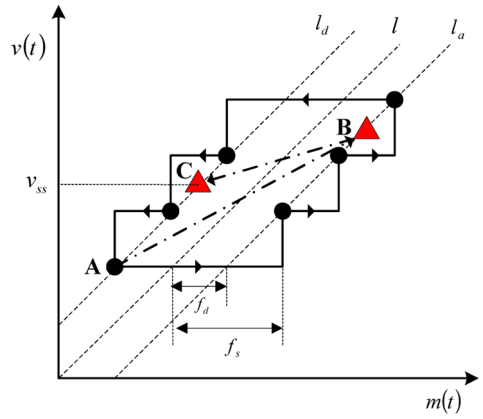

Figure 3. Characterization of the stiction model proposed by He et al.[17] and the path "ABC" of the two valve movements in the proposed compensation methods.

The main idea of the proposed closed-loop compensation method is to add a short-time rectangular wave to the reference $r(t)$ so that the control valve stays at the desired position v_{ss} after two movements, with the control loop operating in the auto mode. The two movements are illustrated via Figure 3: Suppose that the valve currently stays at position "A". Then, the first movement in the compensation is to move the valve from A to position "B", and the second movement from B to the position "C" that is associated with the desired steady-state value v_{ss}. The variation of $m(t)$ in each movement has to be large enough to overcome the effect of stiction in order to move the control valve.

The main idea is also illustrated by showing in Figure 4 the signals $r(t)$, $y_m(t)$, $m(t)$, and $v(t)$ during the compensation. For clarity, Figure 5 presents an enlarged viewpoint of some parts of the signals in Figure 4, around a few specific time instants defined as follows. Let t_A be the time instant the one sample before starting the compensation. The other time instants are

$$\begin{cases} t_B := t_A + T_s \\ t_C := t_B + \theta \\ t_D := t_B + T \\ t_E := t_D + T_s \\ t_F := t_E + \theta \end{cases} \tag{6}$$

where T_s is the sampling period, θ is the time delay in eq 2, and T is the duration of the short-time rectangular wave. Without loss of generality, t_A can be chosen somewhere when $m(t)$ is increasing. At the time instant t_B, the short-time rectangular wave with amplitude r_c and duration T is added into $r(t)$ to make the control valve jump to a new position $v(t_B)$. The valve $v(t)$ stays at the position $v(t_B)$ during the stage $t \in [t_B, t_D]$ for the duration T. The reference $r(t)$ goes back to the normal value at the time instant t_E, and the valve $v(t)$ moves to the desired steady-state value v_{ss} and stays at this value ever since. Therefore, the reference $r(t)$ can be represented as

$$r(t) = r_0\mathbf{u}(t) + r_c(\mathbf{u}(t - t_B) - \mathbf{u}(t - t_B - T)), \qquad \forall\, t \tag{7}$$

where $\mathbf{u}(t)$ is the unit step signal and r_0 is the desired reference value.

The design parameters are the time instant t_A, the amplitude r_c, and duration T. The design requires a detailed analysis of the signals $y(t)$ ($y_m(t)$), $m(t)$, and $v(t)$, which is given in the next subsection.

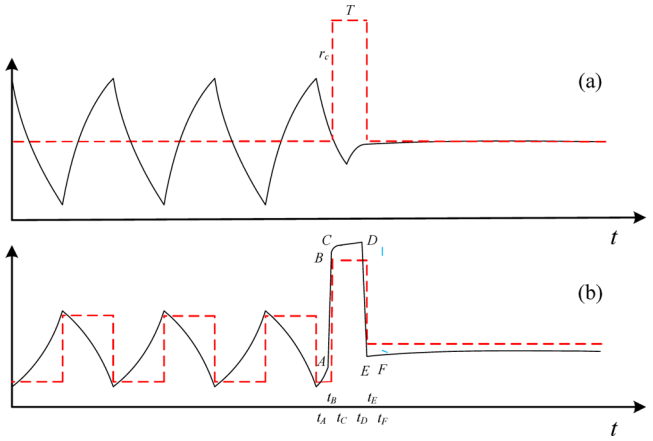

Figure 4. Signals for closed-loop compensation method: (a) measured process output $y_m(t)$ (solid) and reference $r(t)$ (dash), (b) controller output $m(t)$ (solid), and valve output $v(t)$ (dash).

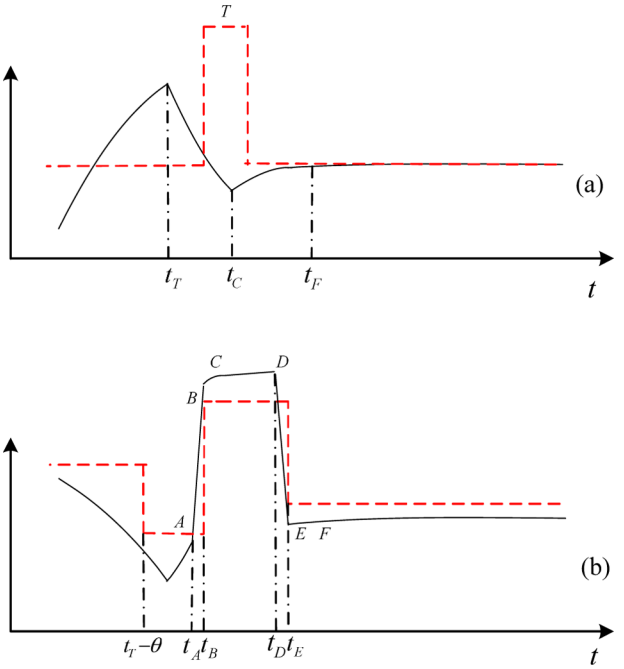

Figure 5. Enlarged signals for closed-loop compensation method: (a) measured process output $y_m(t)$ (solid) and reference $r(t)$ (dash), (b) controller output $m(t)$ (solid), and valve output $v(t)$ (dash).

3.2. Signals at Different Stages. The compensation process consists of several stages denoted by ABCDEF in Figure 4. This subsection analyzes the signals $y(t)$ ($y_m(t)$), $m(t)$, and $v(t)$ for each stage.

Stages AB and BC. Recall that t_A is defined as the time instant the one sample before starting the compensation, while $m(t)$ is increasing. Let t_T be the latest time instant before t_A that $y_m(t)$ changes the direction from increment to decrement. Then, the valve position $v(t)$ at the time instant t_T is, $v(t_T - \theta) = m(t_T - \theta) + f_d$, according to the flowchart of the stiction model in Figure 2. If the variation of $m(t)$ in the time duration from $t_T - \theta + T_s$ to t_A is small such that the inequality $m(t_A) - m(t_T - \theta + T_s) - f_d < f_s$ is satisfied, then the valve position $v(t)$ for $t \in [t_T - \theta, t_A]$ does not move and stays at the value $m(t_T - \theta) + f_d$. Hence, owing to the time delay θ, the process output $y(t)$ during the time slot $t \in [t_A, t_C]$ (t_C defined in eq 6) is under open-loop control

dx.doi.org/10.1021/ie400308z | Ind. Eng. Chem. Res. 2013, 52, 13006−13019

at a constant input value $m(t_T - \theta) + f_d$. On the basis of the process model eq 2, $y(t)$ for $[t_A, t_C]$, denoted as $y_{AC}(t)$, can be described as

$$y_{AC}^{(1)}(t) = \frac{K_p}{T_p}(m(t_T - \theta) + f_d) - \frac{1}{T_p}y_{AC}(t) \tag{8}$$

Here the superscript (1) denotes the first-order derivative. Considering the nonzero initial value of $y(t)$ at t_A, the Laplace transformation of eq 8 is

$$sY_{AC}(s) - y(t_A) = \frac{K_p(m(t_T - \theta) + f_d)}{T_p s} - \frac{1}{T_p}Y_{AC}(s)$$

so that

$$\begin{aligned} Y_{AC}(s) &= \frac{K_p(m(t_T - \theta) + f_d)}{T_p s\left(s + \frac{1}{T_p}\right)} + \frac{y(t_A)}{s + \frac{1}{T_p}} \\ &= \frac{K_p(m(t_T - \theta) + f_d)}{s} \\ &\quad + \frac{y(t_A) - K_p(m(t_T - \theta) + f_d)}{s + \frac{1}{T_p}} \end{aligned} \tag{9}$$

The time domain representation of $y_{AC}(t)$ is obtained from eq 9,

$$\begin{aligned} y_{AC}(t) &= K_p(m(t_T - \theta) + f_d) + [y(t_A) \\ &\quad - K_p(m(t_T - \theta) + f_d)]e^{-(t-t_A)/T_p}, \qquad t \in [t_A, t_C] \end{aligned} \tag{10}$$

The controller output $m(t)$ for $[t_A, t_C]$, denoted as $m_{AC}(t)$, is obtained as follows. The controller $C(s)$ in eq 3 is associated with a differential equation

$$m_{AC}^{(1)}(t) = K_c e_{AC}^{(1)}(t) + \frac{K_c}{T_i}e_{AC}(t) \tag{11}$$

where $e_{AC}(t)$ stands for the control error $e(t)$ for $[t_A, t_C]$, i.e.,

$$e_{AC}(t) = r(t) - y_{AC}(t) - c$$

Considering the nonzero initial values at t_A, the Laplace transformation of eq 11 is

$$sM_{AC}(s) - m(t_A) = K_c sE_{AC}(s) - K_c e(t_A) + \frac{K_c}{T_i}E_{AC}(s)$$

The time domain counterpart is

$$\begin{aligned} m_{AC}(t) &= m(t_A) - K_c e(t_A) + K_c e_{AC}(t) \\ &\quad + \frac{K_c}{T_i}\int_{t_A}^{t} e_{AC}(\tau)\,d\tau \end{aligned} \tag{12}$$

The values of $m(t)$ at t_B and t_C, to be used later, are obtained from eq 12. Considering the variation of $r(t)$ in eq 7, eq 12 yields

$$\begin{aligned} m(t_B) &= m(t_A) - K_c e(t_A) + K_c e(t_B) + \frac{K_c}{T_i}\int_{t_A}^{t_B} e_{AC}(\tau)\,d\tau \\ &\approx m(t_A) - K_c(r_0 - y(t_A) - c) + K_c(r_0 + r_c - y(t_B) - c) \\ &\quad + \frac{K_c T_s}{T_i}(r_0 - y(t_A) - c) \\ &= C_B + K_c r_c \end{aligned} \tag{13}$$

where

$$C_B := m(t_A) + K_c(y(t_A) - y(t_B)) + \frac{K_c T_s}{T_i}(r_0 - y(t_A) - c)$$

Note that the approximation in eq 13 is owing to the numerical integration, i.e., $\int_{t_A}^{t_B} e_{AC}(\tau)\,d\tau \approx T_s e(t_A) = T_s(r_0 - y(t_A) - c)$. The value $m(t_C)$ can be obtained analogously to eq 13,

$$\begin{aligned} m(t_C) &= m(t_A) - K_c e(t_A) + K_c e(t_C) + \frac{K_c}{T_i}\int_{t_A}^{t_C} e_{AC}(\tau)\,d\tau \\ &\approx m(t_A) - K_c(r_0 - y(t_A) - c) \\ &\quad + K_c(r_0 + r_c - y(t_C) - c) + \frac{K_c T_s}{T_i}[r_0 - y(t_A) - c \\ &\quad + \sum_{t=t_B}^{t_C - T_s}(r_0 + r_c - y_{AC}(t) - c)] \\ &= C_C + K_c r_c + \frac{K_c \theta}{T_i}r_c \end{aligned} \tag{14}$$

where

$$C_C := m(t_A) + K_c(y(t_A) - y(t_C)) + \frac{K_c T_s}{T_i}\sum_{t=t_A}^{t_C - T_s}(r_0 - y_{AC}(t) - c)$$

If the magnitude of r_c is sufficient large, the amplitude change of $r(t)$ at t_B can make the valve move to a new position. As $r(t)$ increases, from eq 5, the new valve position is

$$v(t_B) = m(t_B) - f_d \tag{15}$$

Stages CD, DE, and EF. For certain values of r_c and T, the accumulative variation of $m(t)$ from t_B to t_D is small so that the valve stays with $v(t_B)$ in eq 15, i.e.,

$$v(t) = v(t_B) = m(t_B) - f_d, \qquad \text{for } t \in [t_B, t_D]$$

At the time instant $t_D := t_B + T$, the short-time rectangular wave with amplitude r_c and duration T disappears. However, owing to the time delay θ, the process output $y(t)$ is under open-loop control at a constant input value $v(t_B)$ during the time slot $t \in [t_C, t_F]$ (t_F is defined in eq 6). Thus, $y(t)$ for $[t_C, t_F]$, denoted as $y_{CF}(t)$, can be obtained analogously to $y_{AC}(t)$ in eq 10,

$$\begin{aligned} y_{CF}(t) &= K_p(m(t_B) - f_d) + [y(t_C) \\ &\quad - K_p(m(t_B) - f_d)]e^{-(t-t_C)/T_p}, \qquad t \in [t_C, t_F] \end{aligned} \tag{16}$$

Analogously to $m_{AC}(t)$ in eq 12 $m(t)$ for $t \in [t_C, t_F]$, denoted as $m_{CF}(t)$, is

$$\begin{aligned} m_{CF}(t) &= m(t_C) - K_c e(t_C) + K_c e_{CF}(t) \\ &\quad + \frac{K_c}{T_i}\int_{t_C}^{t} e_{CF}(\tau)\,d\tau \end{aligned} \tag{17}$$

where

$$e_{CF}(t) = r(t) - y_{CF}(t) - c \tag{18}$$

For certain values of r_c and T, the magnitude change of $r(t)$ at t_E is sufficiently large so that the valve moves to a new position

$$v(t_E) = m(t_E) - f_d$$

3.3. Design of r_c and T. On the basis of the analysis of signals in section 3.2, this subsection investigates the design of the parameters r_c and T.

3.3.1. Function between r_c and T to achieve a desired value $m(t_E)$. The valve is expected to arrive at the desired steady-state value v_{ss} at the time instant t_E and stay at this

dx.doi.org/10.1021/ie400308z | Ind. Eng. Chem. Res. 2013, 52, 13006−13019

position ever since. Since $m(t)$ jumps down from $m(t_D)$ to $m(t_E)$, making $v(t)$ arrive at v_{ss} requires

$$m(t_E) = v_{ss} - f_d \tag{19}$$

From $r(t)$ in eq 7, $m_{CF}(t)$ in eq 17 and $e_{CF}(t)$ in eq 18,

$$\begin{aligned} m(t_E) &= m(t_D) - K_c e(t_D) + K_c e(t_E) + \frac{K_c}{T_i}\int_{t_D}^{t_E} e_{CF}(\tau)\,d\tau \\ &\approx m(t_D) - K_c(r_0 + r_c - y(t_D) - c) + K_c(r_0 - y(t_E) - c) \\ &\quad + \frac{K_c}{T_i}T_s(r_0 + r_c - y(t_D) - c) \\ &= m(t_D) - K_c r_c + K_c(y(t_D) - y(t_E)) \\ &\quad + \frac{K_c T_s}{T_i}(r_0 + r_c - y(t_D) - c) \end{aligned} \tag{20}$$

Thus, it is necessary to represent $y(t_D)$, $y(t_E)$, and $m(t_D)$ in eq 20 in terms of the design parameters r_c and T_0. Using $y_{CF}(t)$ in eq 16 and the definition of time instants in eq 6, $y(t_D)$ and $y(t_E)$ are obtained as

$$\begin{aligned} y(t_D) &= K_p(m(t_B) - f_d) + [y(t_C) \\ &\quad - K_p(m(t_B) - f_d)]e^{-(T-\theta)/T_p} \end{aligned} \tag{21}$$

$$\begin{aligned} y(t_E) &= K_p(m(t_B) - f_d) + [y(t_C) \\ &\quad - K_p(m(t_B) - f_d)]e^{-(T-\theta+T_s)/T_p} \end{aligned} \tag{22}$$

With $y_{CF}(t)$ in eq 16, $m_{CF}(t)$ in eq 17 and $y(t_D)$ in eq 21, $m(t_D)$ can be represented as

$$\begin{aligned} m(t_D) &= m(t_C) - K_c e(t_C) + K_c e(t_D) + \frac{K_c}{T_i}\int_{t_C}^{t_D} e_{CD}(\tau)\,d\tau \\ &= m(t_C) + K_c(y(t_C) - y(t_D)) \\ &\quad + \frac{K_c}{T_i}\int_{t_C}^{t_D}(r_0 + r_c - y_{CF}(\tau) - c)\,d\tau \\ &= m(t_C) + \frac{K_c}{T_i}(r_0 + r_c - c)(T - \theta) \\ &\quad + K_c\{y(t_C) - K_p(m(t_B) - f_d) \\ &\quad - [y(t_C) - K_p(m(t_B) - f_d)]e^{-(T-\theta)/T_p}\} \\ &\quad - \frac{K_c}{T_i}\int_{t_C}^{t_D}(K_p(m(t_B) - f_d) \\ &\quad + [y(t_C) - K_p(m(t_B) - f_d)]e^{-(\tau - t_C)/T_p})\,d\tau \\ &= m(t_C) + \frac{K_c}{T_i}[r_0 + r_c - c - K_p(m(t_B) - f_d)] \\ &\quad (T - \theta) + K_c\left(1 - \frac{T_p}{T_i}\right) \\ &\quad [y(t_C) - K_p(m(t_B) - f_d)](1 - e^{-(T-\theta)/T_p}) \end{aligned} \tag{23}$$

Substituting $y(t_D)$ in eq 21, $y(t_E)$ in eq 22, and $m(t_D)$ in eq 23 into eq 20 yields

$$\begin{aligned} m(t_E) &\approx m(t_C) + \frac{K_c}{T_i}[r_0 + r_c - c - K_p(m(t_B) - f_d)](T - \theta) \\ &\quad + K_c\left(1 - \frac{T_p}{T_i}\right)[y(t_C) - K_p(m(t_B) - f_d)](1 - e^{-(T-\theta)/T_p}) \\ &\quad - K_c r_c + K_c[y(t_C) - K_p(m(t_B) - f_d)](e^{-(T-\theta)/T_p} \\ &\quad - e^{-(T-\theta+T_s)/T_p}) + \frac{K_c T_s}{T_i}[r_0 + r_c - K_p(m(t_B) - f_d) - c] \\ &\quad - \frac{K_c T_s}{T_i}[y(t_C) - K_p(m(t_B) - f_d)]e^{-(T-\theta)/T_p} \\ &= m(t_C) + \frac{K_c}{T_i}(T - \theta + T_s)(r_0 - c - y(t_C)) \\ &\quad + \frac{K_c}{T_i}(T - \theta - T_i + T_s)r_c + F_1(T)[y(t_C) - K_p(m(t_B) - f_d)] \end{aligned} \tag{24}$$

where

$$F_1(T) := \frac{K_c}{T_i}[T + T_i + T_s - \theta - T_p + (T_p - T_s - T_i e^{-T_s/T_p})e^{-(T-\theta)/T_p}]$$

Using v_{ss} in eq 4, $m(t_B)$ in eq 13 and $m(t_C)$ in eqs 14, 19, and 24 lead to an approximated equality

$$\begin{aligned} \frac{r_0 - c}{K_p} - f_d &\approx C_C + K_c r_c + \frac{K_c\theta}{T_i}r_c + \frac{K_c}{T_i}(T - \theta - T_i + T_s)r_c \\ &\quad + F_1(T)[y(t_C) - K_p(C_B + K_c r_c - f_d)] \end{aligned} \tag{25}$$

As T takes the value as an integer multiple of T_s, eq 25 is rewritten as

$$\begin{aligned} r_c \approx &\left[\frac{r_0 - c}{K_p} - f_d - C_C - F_1(T)[y(t_C) - K_p(C_B - f_d)]\right. \\ &\left. - \frac{K_c}{T_i}(T - \theta + T_s)(r_0 - c - y(t_C))\right] \\ &/\left[\frac{K_c(T + T_s)}{T_i} - F_1(T)K_p K_c\right] \end{aligned} \tag{26}$$

In words, given a specific value of T, the value of r_c can be determined from the approximated function eq 26, in order to make $v(t_E)$ arrive at v_{ss}. Note that the terms C_B and C_C are irrelevant to r_c.

3.3.2. Conditions To be Satisfied. Besides eq 26, the parameters r_c and T have to satisfy certain conditions to make the valve move in the same way as described in the above stages.

Stage AB. Recall that t_T (defined at the beginning of section 3.2) is the latest time instant that $y(t)$ changes the direction from increment to decrement, before adding the short-time rectangular wave, and $m(t_T - \theta)$ is the value of $m(t)$ to make the latest movement of the valve. According to the flowchart of the stiction model in Figure 2, the valve movement at t_B requires

$$-f_d + m(t_A) - m(t_T - \theta) < f_s \tag{27}$$

and

$$-f_d + m(t_A) - m(t_T - \theta) + m(t_B) - m(t_A) > f_s \tag{28}$$

Equation 27 confines the amplitude of $m(t_A)$, i.e.,

$$m(t_A) < f_s + f_d + m(t_T - \theta) \tag{29}$$

Substituting $m(t_B)$ in eq 13 into eq 28 yields

$$-f_d - m(t_T - \theta) + C_B + K_c r_c \gtrsim f_s$$

dx.doi.org/10.1021/ie400308z | Ind. Eng. Chem. Res. 2013, 52, 13006−13019

so that r_c has a lower bound

$$r_c \gtrsim \frac{f_s + f_d + m(t_T - \theta) - C_B}{K_c} \tag{30}$$

Stage BC. For the stage BC, the valve does not move so that the increment of $m(t)$ needs to satisfy the inequality

$$f_d + m(t_C) - m(t_B) < f_s \tag{31}$$

Substituting $m(t_B)$ in eq 13 and $m(t_C)$ in eq 14 into the inequality eq 31 gives

$$f_d + C_C + K_c r_c + \frac{K_c\theta}{T_i} r_c - (C_B + K_c r_c) \lesssim f_s$$

which imposes an upper bound to r_c

$$r_c \lesssim \frac{f_s - f_d - C_C + C_B}{\frac{K_c\theta}{T_i}} \tag{32}$$

Stage CD. Similar to the stage BC, the valve does not move at the stage CD so that another inequality has to be satisfied

$$f_d + m(t_C) - m(t_B) + m(t_D) - m(t_C) \lesssim f_s \tag{33}$$

On the basis of $m(t_B)$ in eq 13 and $m(t_D)$ in eq 23, the inequality eq 33 becomes

$$f_d + C_C - C_B + \frac{K_c\theta}{T_i} r_c + \frac{K_c}{T_i}[r_0 + r_c - c - K_p(C_B + K_c r_c - f_d)](T - \theta) + K_c\left(1 - \frac{T_p}{T_i}\right)[y(t_C) - K_p(C_B + K_c r_c - f_d)](1 - e^{-(T-\theta)/T_p}) < f_s$$

which gives an upper bound of r_c being dependent on T

$$r_c \lesssim \frac{f_s - f_d - C_C + C_B - \frac{K_c}{T_i}[r_0 - c - K_p(C_B - f_d)](T - \theta) - K_c\left(1 - \frac{T_p}{T_i}\right)[y(t_C) - K_p(C_B - f_d)](1 - e^{-(T-\theta)/T_p})}{\frac{K_c\theta}{T_i} + \frac{K_c}{T_i}(1 - K_pK_c)(T - \theta) - K_c^2K_p\left(1 - \frac{T_p}{T_i}\right)(1 - e^{-(T-\theta)/T_p})} \tag{34}$$

In practice, $m(t)$ is usually confined to be less than an upper limit value, e.g., $m(t) \le 100$. Since $m(t_D)$ in eq 23 is the largest value of $m(t)$ during the compensation, the next inequality holds for an upper limit m_H of $m(t)$

$$m_H \ge m(t_D) = m(t_C) + \frac{K_c}{T_i}[r_0 + r_c - c - K_p(m(t_B) - f_d)](T - \theta) + K_c\left(1 - \frac{T_p}{T_i}\right)[y(t_C) - K_p(m(t_B) - f_d)](1 - e^{-(T-\theta)/T_p})$$

This leads to another upper bound of r_c, by using $m(t_B)$ in eq 13 and $m(t_C)$ in eq 14,

$$r_C \lesssim \frac{m_H - C_C - \frac{K_c}{T_i}(r_0 - c - y(t_C)) - \frac{K_c}{T_i}[y(t_C) - K_p(C_B - f_d)][T - \theta + (T_i - T_p)(1 - e^{-(T-\theta)/T_p})]}{K_c + \frac{K_cT}{T_i} - \frac{K_c^2K_p}{T_i}[(T - \theta) + (T_i - T_p)(1 - e^{-(T-\theta)/T_p})]} \tag{35}$$

Stage DE. In the stage DE, $m(t)$ decreases with a significant magnitude so that the valve moves to a new position. This requires an inequality,

$$f_d + m(t_C) - m(t_B) + m(t_D) - m(t_C) + m(t_E) - m(t_D) < -f_s$$

which becomes, based on $m(t_B)$ in eq 13 and $m(t_E)$ in eq 24,

$$f_d + C_C - C_B + \frac{K_c\theta}{T_i} r_c + \frac{K_c}{T_i}(T - \theta + T_s)(r_0 - c - y(t_C)) + \frac{K_c}{T_i}(T - \theta - T_i + T_s)r_c + F_I(T)[y(t_C) - K_p(C_B + K_c r_c - f_d)] \lesssim -f_s$$

Thus, another lower bound of r_c is obtained

$$r_c \gtrsim \frac{f_s + f_d + C_C - C_B + \frac{K_c}{T_i}(T - \theta + T_s)(r_0 - c - y(t_C)) + F_I(T)[y(t_C) - K_p(C_B - f_d)]}{F_I(T)K_pK_c - \frac{K_c}{T_i}(T - T_i + T_s)} \tag{36}$$

Stage EF. In the stage EF, $m(t_F)$ is smaller than $m(t_E)$, and the valve does not move so that

$$-f_d + m(t_F) - m(t_E) > -f_s \tag{37}$$

With $m_{CF}(t)$ in eq 17,

$$m(t_F) - m(t_E) = -K_c e(t_E) + K_c e(t_F) + \frac{K_c}{T_i}\int_{t_E}^{t_F} e_{CF}(\tau)\,d\tau = K_c(y(t_E) - y(t_F)) + \frac{K_c}{T_i}\int_{t_E}^{t_F}(r_0 - c - y_{CF}(\tau))\,d\tau \tag{38}$$

Using $y_{CF}(t)$ in eq 16 as well as t_E and t_F in eq 6,

dx.doi.org/10.1021/ie400308z | Ind. Eng. Chem. Res. 2013, 52, 13006−13019

$$y(t_F) = K_p(m(t_B) - f_d) + [y(t_C) - K_p(m(t_B) - f_d)]e^{-(T+t_s)/T_P} \quad (39)$$

and the integration in eq 38 becomes

$$\frac{K_c}{T_i}\int_{t_E}^{t_F}(r_0 - c - y_{CF}(\tau))d\tau = \frac{K_c\theta}{T_i}[r_0 - c - K_p(m(t_B) - f_d)] - \frac{K_cT_P}{T_i}[y(t_C) - K_p(m(t_B - f_d)](e^{-(T-\theta+T_s)/T_P} - e^{-(T+T_s)/T_P})$$

Thus, with $y(t_E)$ in eq 22 and $y(t_F)$ in eq 39, eq 38 is rewritten as

$$\begin{aligned} m(t_F) - m(t_E) &= K_c[y(t_C) - K_p(m(t_B) - f_d)](e^{-(T-\theta+T_s)/T_P} - e^{-(T+T_s)/T_P}) + \frac{K_c\theta}{T_i}[r_0 - c - K_p(m(t_B) - f_d)] - \frac{K_cT_P}{T_i}[y(t_C) - K_p(m(t_B) - f_d)](e^{-(T-\theta+T_s)/T_P} - e^{-(T+T_s)/T_P}) \\ &= \frac{K_c\theta}{T_i}(r_0 - c - y(t_C)) + F_2(T)[y(t_C) - K_p(m(t_B) - f_d)] \end{aligned}$$

where

$$F_2(T) = \frac{K_c}{T_i}(T_i - T_P)(e^{-(T-\theta+T_s)/T_P} - e^{-(T+T_s)/T_P}) + \frac{K_c\theta}{T_i}$$

Using $m(t_B)$ in eq 13, eq 37 yields an upper bound of r_c being dependent on T:

$$r_c \lesssim \left[f_s - f_d + \frac{K_c\theta}{T_i}(r_0 - c - y(t_C)) + F_2(T)[y(t_C) - K_p(C_B - f_d)]\right]/[F_2(T)K_pK_c] \quad (40)$$

3.4. Selection of t_A. Besides the parameters r_c and T, the time instant t_A is another design parameter to be selected. The selection of t_A determines the values of $m(t_A)$ and $y_m(t_A)$ so that the selection affects eq 26, as well as the four upper bounds of r_c in eqs 32, 34, 35 and 40, and the two lower bounds of r_c in eqs 30 and 36.

To achieve a good compensation performance, it is preferred that $y_m(t)$ is equal to the desired steady-state value r_0, right after the disappearance of the short-time rectangular wave, i.e.,

$$y(t_F) = r_0 - c \quad (41)$$

Using $m(t_B)$ in eq 13 and $y(t_F)$ in eq 39, eq 41 becomes

$$\begin{aligned} r_0 - cr_0 - c &= K_p(m(t_B) - f_d) + [y(t_C) - K_p(m(t_B) - f_d)]e^{-(T+T_s)/T_P} \\ &\approx K_p(C_B + K_cr_c - f_d) + [y(t_C) - K_p(C_B + K_cr_c - f_d)]e^{-(T+T_s)/T_P} \\ &= K_pK_cr_c(1 - e^{-(T+T_s)/T_P}) + y(t_C) - [y(t_C) - K_p(C_B - f_d)](1 - e^{-(T+T_s)/T_P}) \end{aligned}$$

which leads to another function between r_c and T

$$r_c \approx \frac{r_0 - c - y(t_C) + [y(t_C) - K_p(C_B - f_d)](1 - e^{-(T+T_s)/T_P})}{K_pK_c(1 - e^{-(T+T_s)/T_P})} \quad (42)$$

Hence, it is desirable to select t_A and T such that r_c from eq 26 and that from eq 42 are close to each other.

3.5. Compensation Steps. The closed-loop compensation method consists of the following steps. The flowchart of these steps is given in Figure 6.

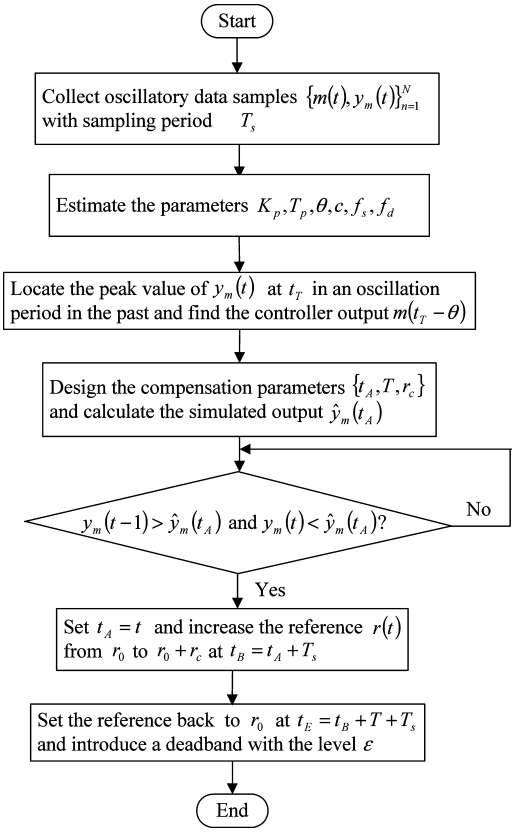

Figure 6. Flowchart for the online implementation of the proposed compensation method.

S1. Estimate the parameters K_p, T_p, θ, c, f_s, and f_d based on the oscillatory data samples $\{y_m(t), m(t)\}_{t=1}^N$.

S2. Locate the time instant t_T in an oscillation period in the past at which $y_m(t)$ changes the direction from increment to decrement, and find the corresponding value $m(t_T - \theta)$ from the current available oscillatory data of $m(t)$ and $y_m(t)$.

S3. For each candidate of $t_A = t_T + lT_s$ for $l = 1, 2, \cdots$, calculate r_c from eq 26 and that from eq 42 for a sequence of T with $T = \theta + kT_s$ for $k = 0, 1, 2, \cdots$. The resulting two groups of sets are denoted as $\{t_A, T, r_c\}_{(26)}$ and $\{t_A, T, r_c\}_{(42)}$, respectively. Find the valid sets satisfying the upper bound of $m(t_A)$ in eq 29, the two lower bounds of r_c in eqs 30 and 36, and the four upper bounds of r_c in eqs 32, 34, 35, and eq 40. Among the valid sets of $\{t_A, T, r_c\}_{(26)}$, select the set whose r_c has the minimal distance with that from $\{t_A, T, r_c\}_{(42)}$ as the optimal choice and calculate the simulated output $\hat{y}_m(t_A)$ via eq 49 (appears later in section 3.6).

S4. Set t_A as the time instant that the two inequalities in eq 43 are satisfied

dx.doi.org/10.1021/ie400308z | Ind. Eng. Chem. Res. 2013, 52, 13006−13019

$$y_m(t-1) > \hat{y}_m(t_A) \quad \text{and} \quad y_m(t) < \hat{y}_m(t_A) \tag{43}$$

and increase the value of the reference $r(t)$ from r_0 to $r_0 + r_c$ at the time instant $t_B := t_A + T_s$.

S5. Decrease the value of $r(t)$ back to the original value r_0 at the time instant $t_E := t_B + T + T_s$ and introduce a deadband with the level ε to the controller at t_E to ignore control control errors having small absolute values. That is, the input to the controller $C(s)$ becomes the output $e_\varepsilon(t)$ of the deadband

$$e_\varepsilon(t) = \begin{cases} e(t), & |e(t)| \geq \varepsilon \\ 0, & |e(t)| < \varepsilon \end{cases} \tag{44}$$

The steps S1−S3 determine the design parameters $\{t_A, T, r_c\}$ based on the past oscillatory data samples of $y_m(t)$ and $m(t)$. Note that the time instant t_T can be selected as the peak value of $y_m(t)$ in any oscillation period in the past, so that the values of $m(t_A)$ and $y_m(t_A)$ are available for the design. Once t_A is determined, the simulated output $\hat{y}_m(t_A)$ is obtained, and the time instant that the two inequalities in eq 43 are satisfied is set to be the actual time instant t_A for the online implementation steps S4 and S5. Thus, the final design parameters for the proposed compensation method are $\{\hat{y}_m(t_A), r_c, T\}$.

3.6. Implementation Issues. This subsection discusses the implementation issues for the proposed compensation methods, namely, the estimation of required parameters and the determination of the deadband level ε.

First, the closed-loop compensation method requires the information of the process parameters K_p, T_p, and θ in eq 2, the constant parameter c (see Figure 1), the controller parameters K_c and T_i in eq 3, and the parameters f_s and f_d of the stiction model in Figure 2. With the exception of the controller parameters K_c and T_i, the other parameters may not be available a priori.

There exist a few approaches in the literature for identification of the required process and stiction models. Srinivasan et al.[19] applied the idea of separable least-squares method to stiction models parametrized by one parameter for control valves. The same idea was generalized by Jelali,[20] Choudhury et al.,[21] Karra and Karim,[22] and Farenzena and Trierweiler[23] to identify Hammerstein systems consisting of a two-parameter stiction model connected with a linear process model.

In this context, the parameters K_p, T_p, and θ in eq 2, the constant parameter c and the parameters f_s and f_d of the stiction model are estimated based on the measurements of $m(t)$ and $y_m(t)$ via a two-step approach. The first step takes the idea of the separable least-squares method, analogous to the two-stage method proposed by Jelali,[20] to estimate the parameters f_s and f_d of the stiction model, and a discrete-time autoregression with extra input (ARX) model for the linear process, i.e.,

$$y_m(t) = -\sum_{i=1}^{n_a} a_i y_m(t-i) + \sum_{j=1}^{n_b} b_j v(t-j-n_k) + d + e(t) \tag{45}$$

It is a well-known fact that the estimation of ARX models only requires the standard linear least-squares method, and a high-order ARX model is capable of approximating any LTI dynamic systems arbitrarily well[24] (page 336). A high-order ARX model can yield very accurate model estimation even if the measurement noise is heavily colored.[25,26] With the estimates $\hat{f}_s$ and $\hat{f}_d$, the estimate of $v(t)$ can be obtained from the He's stiction model depicted in Figure 2 driven by $m(t)$, i.e.,

$$v(t; \hat{f}_s, \hat{f}_d) = f(m(t); \hat{f}_s, \hat{f}_d)$$

Replacing $v(t)$ by $v(t; \hat{f}_s, \hat{f}_d)$, eq 45 becomes

$$y_m(t) = \varphi^T(t; \hat{f}_s, \hat{f}_d)\gamma + e(t)$$

where

$$\varphi(t; \hat{f}_s, \hat{f}_d) = \begin{bmatrix} -y_m(t-1) \\ \vdots \\ -y_m(t-n_a) \\ \hat{v}(t-1-n_k; \hat{f}_s, \hat{f}_d) \\ \vdots \\ \hat{v}(t-n_b-n_k; \hat{f}_s, \hat{f}_d) \\ 1 \end{bmatrix}, \qquad \gamma = \begin{bmatrix} a_1 \\ \vdots \\ a_{n_a} \\ b_1 \\ \vdots \\ b_{n_b} \\ d \end{bmatrix}$$

Given the data samples $\{y_m(t), m(t)\}_{t=1}^N$, the parameter vector γ can be estimated via the least-squares method as

$$\hat{\gamma}(\hat{f}_s, \hat{f}_d) = (\Phi^T(\hat{f}_s, \hat{f}_d)\Phi(\hat{f}_s, \hat{f}_d))^{-1}(\Phi^T(\hat{f}_s, \hat{f}_d)Y_m) \tag{46}$$

where

$$Y_m = \begin{bmatrix} y_m(1) \\ \vdots \\ y_m(N) \end{bmatrix}, \qquad \Phi(\hat{f}_s, \hat{f}_d) = \begin{bmatrix} \varphi^T(1; \hat{f}_s, \hat{f}_d) \\ \vdots \\ \varphi^T(N; \hat{f}_s, \hat{f}_d) \end{bmatrix}$$

The model structure parameters (n_a, n_b, n_k) and the optimal estimates of f_s and f_d are obtained as the ones achieving the minimum value of a loss function associated with the simulation errors, i.e.,

$$(\hat{n}_a^{op}, \hat{n}_b^{op}, \hat{n}_k^{op}, \hat{f}_s^{op}, \hat{f}_d^{op}) = \arg \min_{n_a, n_b, n_k, \hat{f}_s, \hat{f}_d} \frac{1}{N} \sum_{t=1}^{N} (y_m(t) - \varphi^T(t; \hat{f}_s, \hat{f}_d)\hat{\gamma}(\hat{f}_s, \hat{f}_d))^2 \tag{47}$$

The optimization in eq 47 can be solved, e.g., by the global optimization via a grid search over five dimensional space of n_a, n_b, n_k, $\hat{f}_s$, and $\hat{f}_d$. With $\hat{f}_s^{op}$ and $\hat{f}_d^{op}$ in eq 47, the optimal estimate of γ is obtained as $\hat{\gamma}(\hat{f}_s^{op}, \hat{f}_d^{op})$ from eq 46.

The second step is to estimate the parameters K_p, T_p, and θ of the continuous-time model $G(s)$ in eq 2 and the constant parameter c based on the identified discrete-time ARX model denoted as $\hat{G}(q)$. If the step response of $\hat{G}(q)$ reveals whether a FOPTD model can describe the process well, then the estimate of $G(s)$ can be obtained by applying the prediction-error method (PEM)[27] to the step response of $\hat{G}(q)$ (see, e.g., the Matlab function "pem"). Note that the delay parameter θ needs to be estimated as an integer multiple of the sampling period. The constant parameter c is estimated based on the parameters $\hat{a}_i$ and $\hat{d}$ in $\hat{\gamma}(\hat{f}_s^{op}, \hat{f}_d^{op})$ as

$$\hat{c} = \frac{\hat{d}}{1 + \sum_{i=1}^{\hat{n}_a^{op}} \hat{a}_i}$$

dx.doi.org/10.1021/ie400308z | Ind. Eng. Chem. Res. 2013, 52, 13006−13019

The quality of the estimated parameters can be quantitatively measured by the fitness between the measured output $y_m(t)$ and the simulated one $\hat{y}_m(t)$,

$$\text{fitness} = 100\left(1 - \frac{\|\hat{y}_m(t) - y_m(t)\|_2}{\|y_m(t) - E\{y_m(t)\}\|_2}\right) \quad (48)$$

where, $\|\cdot\|_2$ is the Euclidean norm and $\hat{y}_m(t)$ is obtained as

$$\hat{y}_m(t) = \frac{\hat{K}_p e^{-\hat{\theta}s}}{\hat{T}_p s + 1} f(m(t); \hat{f}_s, \hat{f}_d) \quad (49)$$

Second, it is unavoidable that the estimated parameters are associated with modeling errors, and the process noise/disturbance $w(t)$ is present. As a result, the selected set of $\{r_c, T\}$ from eqs 26 and 42 would be deviated from the actual one, so are the lower bounds of r_c in eqs 30 and 36 and the upper bounds of r_c in eqs 32, 34, 35 and 40. Even so, there may still be some space from the selected value r_c to the actual lower and upper bounds. Thus, the two movements of $v(t)$ could be reached as designed, subject to modeling errors and/or process noises. Experimental and numerical illustrations are provided later in examples 1 and 2 in section 4.

With the modeling errors and process noises, the main concern is that $v(t)$ after compensation may stay at a position not exactly equal to v_{ss}, leading to nonzero control errors between $r(t)$ and $y_m(t)$. In this case, the integral action of the PI controller would drive the valve to move again, so that the closed-control loop goes back to oscillations. This problem can be solved by using the deadband in eq 44 to freeze the output of the PI controller $C(s)$ when the absolute value of the control error is small. The deadband is usually available in most industrial distributed control systems (DCSs) and has been commonly used in practice, e.g., the fourth suggestion made by Gerry and Ruel.[5] The deadband level ε in eq 44 is chosen to be proportional to the sample standard deviation of the estimated process noise $\hat{w}(t) := y_m(t) - \hat{y}_m(t)$, i.e.,

$$\varepsilon = 3\sqrt{\frac{1}{N-1}\sum_{t=1}^{N}\left(\hat{w}(t) - \frac{1}{N}\sum_{t=1}^{N}\hat{w}(t)\right)^2} \quad (50)$$

4. EXAMPLES

This section provides laboratory and simulation examples to illustrate the proposed closed-loop compensation method and to compare with two existing compensation methods.

Example 1. A laboratory experiment is carried out at Peking University, with the experiment configuration schematically depicted in Figure 7. In the experiment, the linear process is a water tank system, whose cross-sectional area is about 320 cm^2. The opening position of the outlet valve is fixed. The water level of the tank system is controlled by adjusting the inlet flow via a control valve driven by a proportional−integral (PI) controller,

$$C(s) = 0.25\left(1 + \frac{1}{50s}\right) \quad (51)$$

The discrete-time counterpart of the PI controller $C(s)$ is implemented with the sampling period 0.5 s in a DCS platform of Siemens PCS7. Thus, the closed-control loop depicted in Figure 1 is formulated, where $y_m(t)$, $m(t)$, and $r(t)$ stand for the water level of the tank system, the controller output, and the reference, respectively. The stiction is increased by tightening the valve stem packing screw. As a result, $y_m(t)$ and $m(t)$ shown in Figure 8 are oscillatory due to the control valve stiction, even if the reference $r(t)$ is kept at a constant value $r_0 = 35$ and no external disturbance other than measurement noise is present as $w(t)$ in Figure 1. Note that the valve position $v(t)$ in Figure 8 is available in the experiment, but it is used only for validation, not for estimating the parameters of process and stiction models. [The data and identified models for the experiments are available for academic studies: http://www.mech.pku.edu.cn/robot/teacher/wangjiandong/research.htm.]

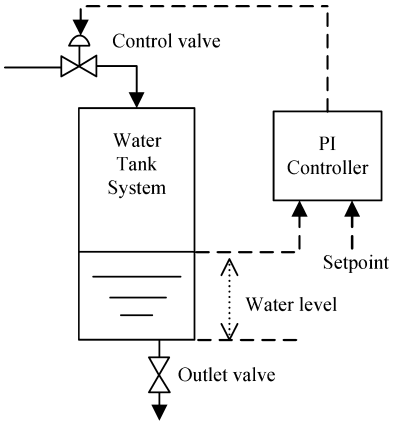

Figure 7. Diagram of the feedback control loop for a water tank system.

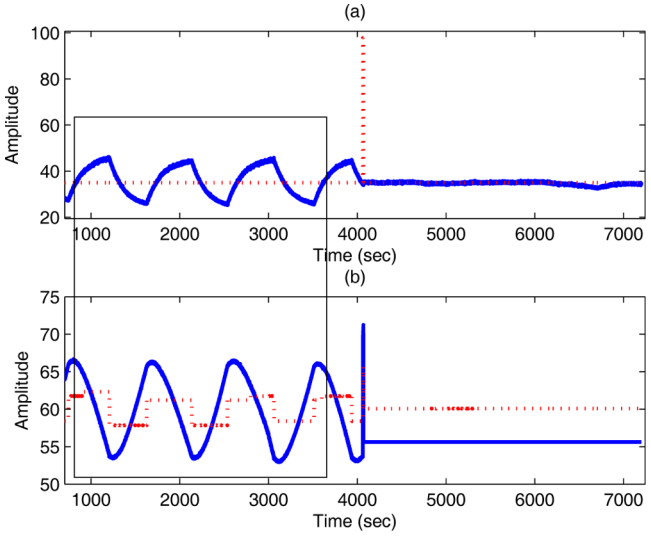

Figure 8. Signals in example 1: (a) $y_m(t)$ (solid) and $r(t)$ (dash), (b) $m(t)$ (solid), and $v(t)$ (dash).

First, based on the oscillatory data samples $\{y_m(t), m(t)\}_{t=1600}^{7200}$ (inside the rectangular box in Figure 8 and represented in Figure 12), the two-step approach in section 3.6 is exploited to yield an ARX model $\hat{G}(q)$ with the structure parameters $\hat{n}_a^{op} = 5$, $\hat{n}_b^{op} = 5$, and $\hat{n}_k^{op} = 1$. From the step response of $\hat{G}(q)$ shown in Figure 9, the process model is identified,

$$\hat{G}(s) = \frac{3.8163}{156.46s + 1} e^{-2.5s} \quad (52)$$

As shown in Figure 9, the step response of $\hat{G}(s)$ fits well with that of $\hat{G}(q)$, except for a few points at the beginning stage of

dx.doi.org/10.1021/ie400308z | Ind. Eng. Chem. Res. 2013, 52, 13006−13019

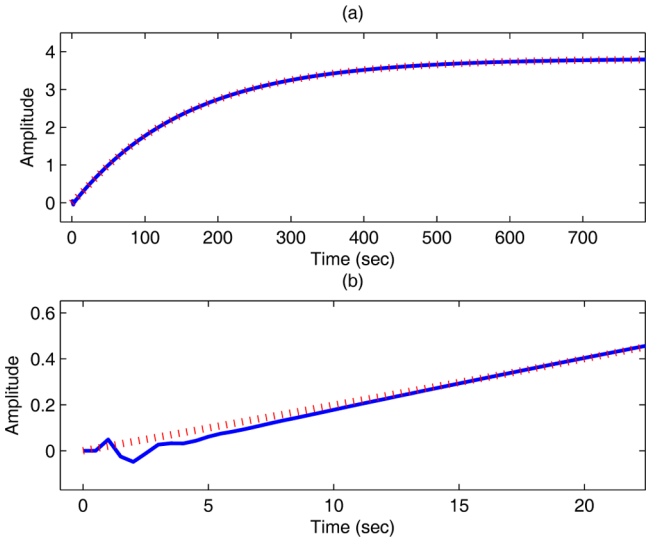

Figure 9. Step responses of the identified models $\hat{G}(q)$ (solid) and $\hat{G}(s)$ (dash) in example 1: (a) the entire step responses and (b) the enlarged parts for the beginning stage of the step responses.

the step responses. The constant parameter c (see Figure 1) and the parameters f_s and f_d for the stiction model are estimated

$$\hat{c} = -192.3411, \qquad \hat{f}_s = 8.4, \qquad \hat{f}_d = 3.5243 \tag{53}$$

Here the valve position $v(t)$ is available so that the estimated parameters $\hat{f}_s$ and $\hat{f}_d$ in eq 53 can be validated from a valve signature obtained by plotting $m(t)$ vs $v(t)$ in Figure 10, where

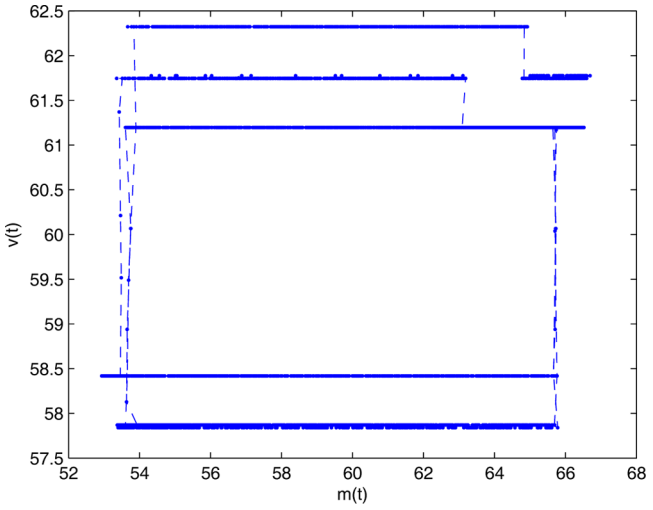

Figure 10. Valve signature $m(t)$ vs $v(t)$ in example 1.

the horizontal and vertical lines have the lengths close to $(\hat{f}_s + \hat{f}_d)$ and $(\hat{f}_s - \hat{f}_d)$, respectively (see also Figure 3). Figure 11 also compares the measured valve position $v(t)$ and its estimate $\hat{v}(t)$ from the identified He's stiction model using $\hat{f}_s$ and $\hat{f}_d$ in eq 53. The He's stiction model is a close approximation of the actual valve character, despite some minor discrepancy between $v(t)$ and $\hat{v}(t)$ in Figure 11. In practice, the measurement of $v(t)$ is usually unavailable, and the validation of the identified models can rely on the comparison between the measured output $y_m(t)$ and the simulated output $\hat{y}_m(t)$ obtained via eq 49. As shown in Figure 12a, $\hat{y}_m(t)$ can well capture the main dynamic variation of $y_m(t)$, with the

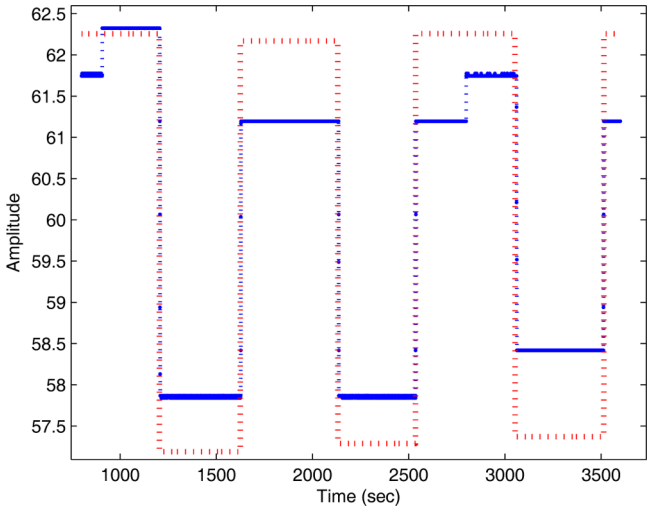

Figure 11. Measured valve position $v(t)$ (solid) and its estimate $\hat{v}(t)$ (dash) in example 1 (solid).

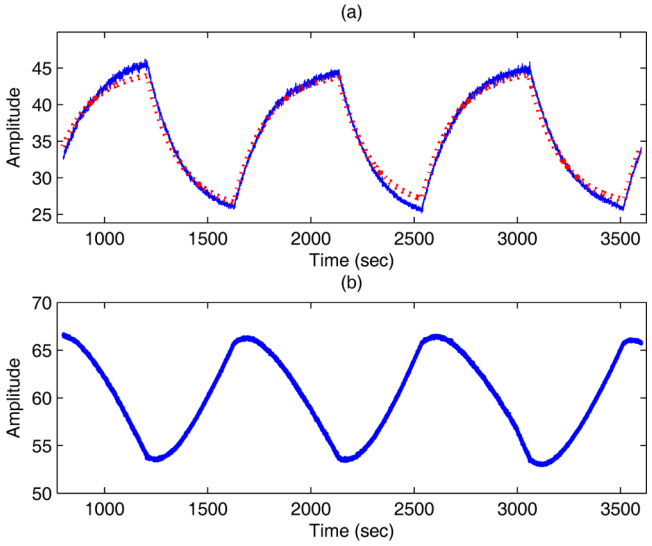

Figure 12. Oscillatory data samples for model identification in example 1: (a) $y_m(t)$ (solid) and $\hat{y}_m(t)$ (dash), (b) $m(t)$ (solid).

fitness in eq 48 equal to 87.6257%. Hence, the estimated parameters of the process and stiction models are satisfactory.

Second, the design parameters for the proposed compensation method are determined. The last peak value of the data segment $y_m(t)$ shown in Figure 12 is selected as the sample $y_m(t_T)$, i.e., t_T = 3058 s. Using the estimate of θ equal to 2.5 s in eq 52, $m(t_T - \theta)$ = 53.7115 is obtained from the available samples of $m(t)$. The optimal choice of t_A leads to $m(t_A)$ = 53.9650 and $y_m(t_A)$ = 33.9999, and the design parameters for online implementation of the proposed compensation method,

$$\hat{y}_m(t_A) = 34, \qquad T = 6.5 \text{ s}, \qquad r_c = 62.7585 \tag{54}$$

Figure 13 presents the optimal choice of $\{r_c, T\}$, denoted by the symbol "*", as well as the associated two functions in eqs 26 and 42, two lower bounds of r_c in eqs 30 and 36, and two upper bounds of r_c in eqs 34 and 35. Note that the other two upper bounds of r_c in eq 32 and eq 40 are far away from the optimal choice and thus are not shown in Figure 13. The deadband level ε is calculated from eq 50, ε = 3.2.

dx.doi.org/10.1021/ie400308z | Ind. Eng. Chem. Res. 2013, 52, 13006−13019

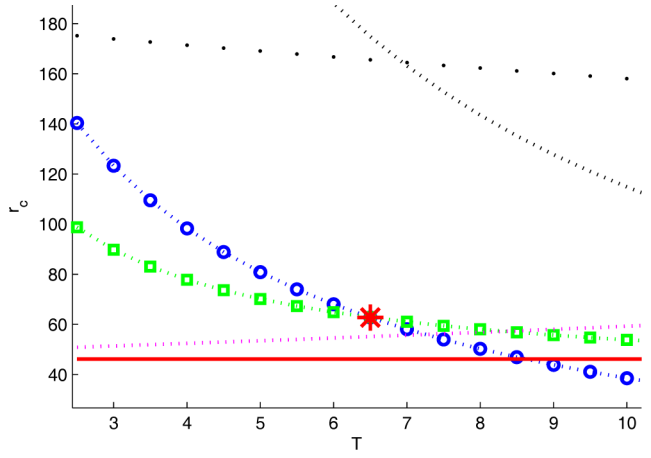

Figure 13. Design for example 1. The functions in eq 26 (circle−dash line) and eq 42 (square−dash line), the lower bounds of r_c in eq 30 (solid line) and eq 36 (dash line at the bottom), and the upper bounds of r_c in eq 34 (dash line at the right-upper corner) and eq 35 (dotted line).

Next, the proposed compensation method is implemented in an online manner, as depicted in the flowchart in Figure 6. That is, when the two inequalities in eq 43 are satisfied, then the short-time rectangular wave is added to the reference $r(t)$ at the next sample. Figure 8 shows the signals before and after the compensation. Figure 14 presents an enlarged vision of signals

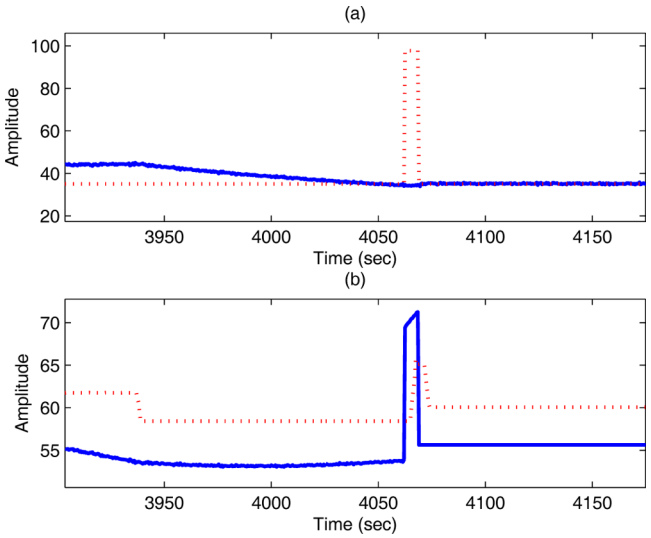

Figure 14. Enlarged vision of signals at the stage of adding the short-time rectangular wave to $r(t)$ in the laboratory example 1: (a) $y_m(t)$ (solid) and $r(t)$ (dash), (b) $m(t)$ (solid) and $v(t)$ (dash).

at the stage of adding the short-time rectangular wave to $r(t)$. As expected, the valve position stays at a desired position so that the water level $y_m(t)$ is close to the desired reference value $r_0 = 35$, and the oscillation disappears after compensation.

Finally, if the reference $r(t)$ experiences a variation or a load disturbance (as $w(t)$ in Figure 1) being additive to the process output $y_m(t)$ is present, then the closed-loop loop after compensation like that in Figure 8 may go back to oscillations. In this case, the proposed compensation method can be applied again to remove the oscillations. As an illustration, another inlet flow controlled by a frequency converter is injected to the water tank system to induce a step load disturbance $w(t)$. Figure 15c presents the step change of the command to the frequency converter and the variation of the corresponding inlet flow. As a result, the load disturbance leads to the reappearance of oscillations, as shown in Figure 15. In order to remove the reappeared oscillations, the design parameters for the proposed compensation method can be determined analogously to those in eq 54. By assuming that the process model in eq 52 and the parameters f_s and f_d in eq 53 are kept the same, the constant parameter c needs to be updated by comparing the measured process output and the simulated one $\hat{y}_m(t)$ in eq 49, based on the oscillatory data samples $\{y_m(t),\ m(t)\}_{t=7919}^{10584}$ (inside the rectangular box in 15), namely, $\hat{c} = -95.9611$. The optimal design parameters are determined as

$$\hat{y}_m(t_A) = 33.5291, \qquad T = 8.5\ \text{s}, \qquad r_c = 70.8218 \tag{55}$$

As expected, using these design parameters, the online implementation of the proposed compensation method removes the oscillations as shown in Figure 15. Here the same deadband level $\varepsilon = 3.2$ is used.

In example 1, even though both the modeling error and measurement noise are present as revealed in Figure 12, the proposed compensation method still achieves satisfactory results. That is, the original oscillation disappears and the process output is close to the desired reference value after compensation. A simulation example is provided next, in order to further explain the rationale stated in section 3.6 for the proposed method having a certain level of robustness against modeling errors and measurement noises.

Example 2. A simulation experiment is performed for the closed-control loop depicted in Figure 1, where the PI controller $C(s)$, the process model $G(s)$, the constant parameter c, and the parameters f_s, f_d for the stiction model are the same as those in eqs 51, 52 and 53 in example 1, respectively. In other words, the estimated parameters of the process and stiction models are regarded as the actual ones in this simulation example. The measurement noise $w(t)$ is absent. The rest configuration is the same as example 1.

A modeling error in terms of the time delay θ is considered. That is, a biased value of the time delay $\theta = 5$ s, instead of the actual one $\theta = 2.5$ s in eq 52, is used for the design of the proposed compensation method. As a result, the designed parameters become

$$\hat{y}_m(t_A) = 34, \qquad T = 5\ \text{s}, \qquad r_c = 73.1708 \tag{56}$$

Figure 16 is the counterpart of Figure 13. Note that the axes of Figure 16 are set to be the same as those of Figure 13 for comparison purpose, and the minimum value of T starts from the time delay $\theta = 5$ s in Figure 16. The optimal choice of $\{r_c, T\}$ in eq 56, denoted by the symbol "*" in Figure 16, is different from that in eq 54 (the symbol "*" in Figure 13). However, there is quite a large space from the optimal choice of r_c in Figure 16 to the actual lower and upper bounds in Figure 13. Hence, the two movements of $v(t)$ can be reached as designed, which is validated by the compensation result shown in Figure 17. Due to the modeling error in θ, the valve position in Figure 17 after compensation stays at $v(t) = 59.1604$, being different from the desired position $v_{ss} = (r_0 - c)/K_p = 59.5711$. Thus, the process output after compensation has a small deviation from the desired reference value r_0. The deadband with $\varepsilon = 3.2$ (the same as example 1) tolerates such a small deviation and freezes the output of the PI controller, as shown in Figure 17.

The next two simulation examples compare the proposed closed-loop compensation method with the method proposed

dx.doi.org/10.1021/ie400308z | Ind. Eng. Chem. Res. 2013, 52, 13006−13019

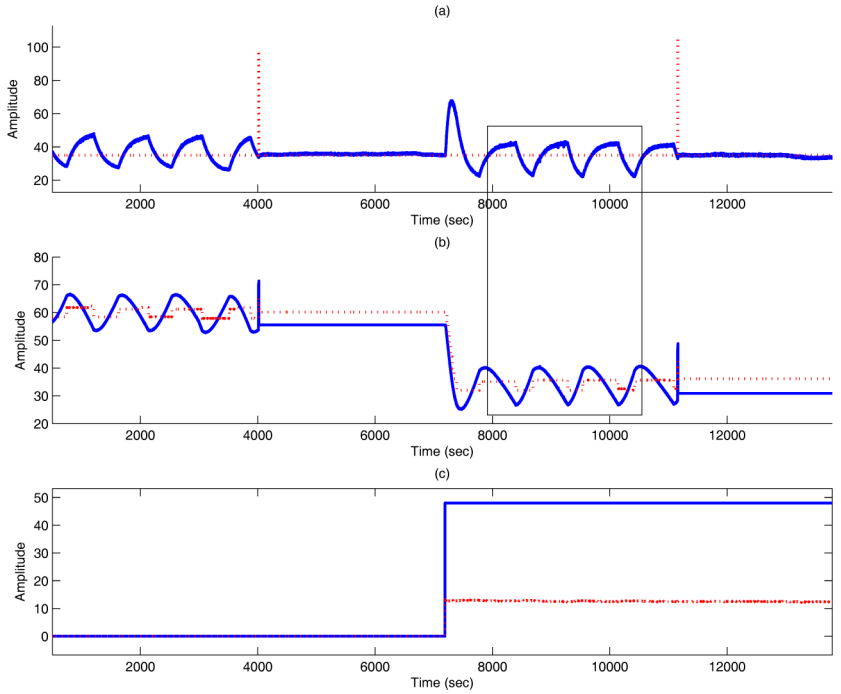

Figure 15. Signals in the laboratory example 1 with a load disturbance: (a) $y_m(t)$ (solid) and $r(t)$ (dash), (b) $m(t)$ (solid) and $v(t)$ (dash), (c) the command to the frequency converter (solid) and the variation of the corresponding inlet flow (dash).

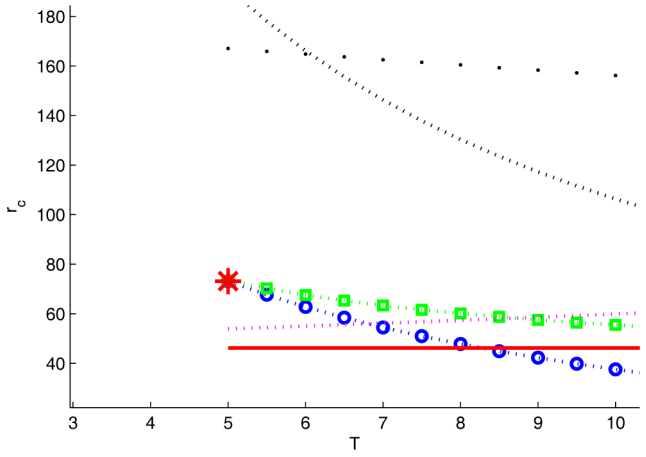

Figure 16. Design for example 2 with a modeling error in the time delay: eq 26 (circle−dash line) and eq 42 (square−dash line), the lower bounds of r_c in eqs 30 (solid line) and 36 (dash line at the bottom), and the upper bounds of r_c in eq 34 (dash line at the right-upper corner) and eq 35 (dotted line).

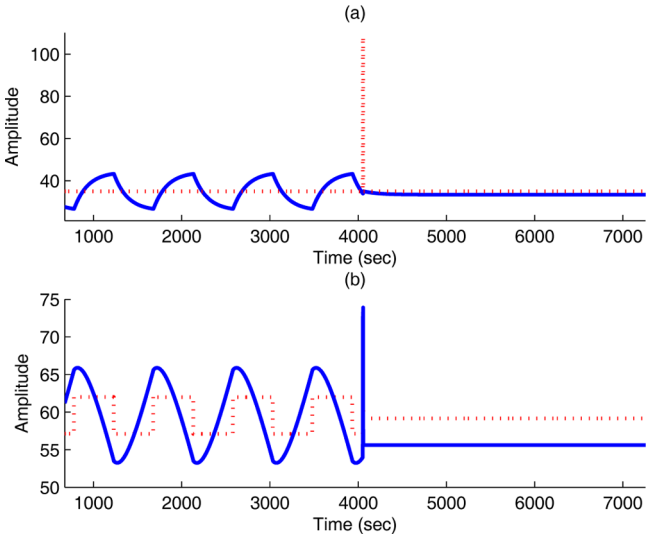

Figure 17. Signals in example 2: (a) $y_m(t)$ (solid) and $r(t)$ (dash), (b) $m(t)$ (solid) and $v(t)$ (dash).

by Cuadros et al.[13] and that by Mohammad and Huang,[14] respectively. Analogously to example 2, simulation experiments in examples 3 and 4 are performed for the closed-control loop depicted in Figure 1 by taking the estimated parameters of the process and stiction models as the actual ones. To ease the comparison, the measurement noise $w(t)$ is absent. The rest of the configuration, including the PI controller, is the same as example 1.

Example 3. The compensation method proposed by Cuadros et al.[13] is based on the knocker method,[7] which adds a compensation signal $m_k(t)$ to the controller output $m(t)$, namely,

$$m_k(t) = \begin{cases} \text{asign}(m(t) - m(t_p)), & t \le t_p + h_k + \tau \\ 0, & t > t_p + h_k + \tau \end{cases}$$

By following the guideline given in ref 9, the three parameters are selected as

$$a = 0.5(f_s + f_d) = 5.9622$$

$$\tau = 2T_s = 1, \qquad h_k = 5T_s = 2.5$$

The compensation method[13] disables the PI controller if the variation of a filtered control error $e_f(t)$ is small, i.e., $|de_f(t)/dt| < \delta$ for a small value $\delta = 0.2$, during the time period of $4h_k$. As the noise $w(t)$ is absent, the control error $e(t)$ is used instead of $e_f(t)$. For clarity, the mechanism of disabling the PI controller is set to be active after the knocker has been enabled for a while. The compensation result is given in Figure 18, with some enlarged part in Figure 19. It is revealed from Figure 19 that the knocker method

dx.doi.org/10.1021/ie400308z | Ind. Eng. Chem. Res. 2013, 52, 13006−13019

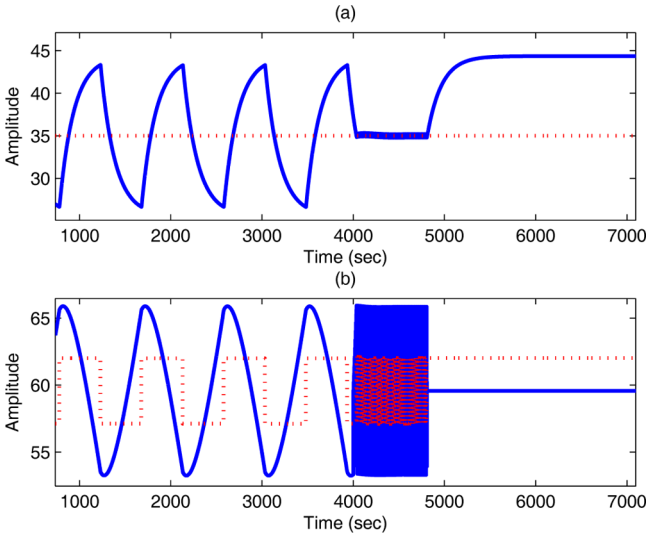

Figure 18. Signals in example 3: (a) $y_m(t)$ (solid) and $r(t)$ (dash), (b) $m(t)$ (solid) and $v(t)$ (dash).

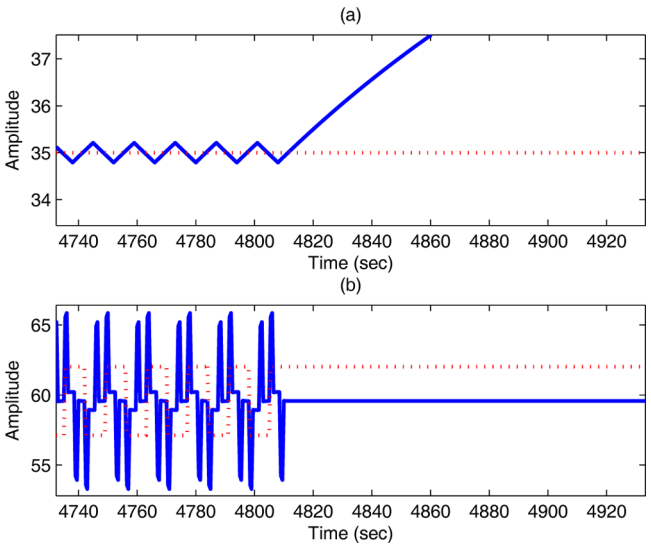

Figure 19. Enlarged vision of signals for example 3: (a) $y_m(t)$ (solid) and $r(t)$ (dash), (b) $m(t)$ (solid) and $v(t)$ (dash).

can reduce the amplitude of oscillation significantly and make the control errors to be small, by fast switching among several control positions. When the mechanism of disabling the PI controller is set to be active, the valve stays a position that is however not guaranteed to be close to the desired valve position. In Figure 19, the valve stays at a position quite far away from the desired one, resulting in a large control error. By contrast, as shown in Figure 8, the proposed compensation method does not result in a sacrifice on the fast variation of valve positions, and the control error is much smaller after compensation.

Example 4. For the FOPDT model in eq 52, the compensation method proposed by Mohammad and Huang[14] says that reducing the integral action can remove the presence of oscillation. Thus, the parameter T_i of $C(s)$ in eq 51 is set to $T_i = 2000$ after the appearance of oscillations, with the parameter $K_c = 0.25$ unchanged. The valve position in Figure 20 after compensation is quite different from the desired position. As a result, the control error is large even if the oscillation disappears after compensation. By contrast, the proposed compensation method moves the valve close to the desired position, so that the control error is much smaller, as shown in Figure 8.

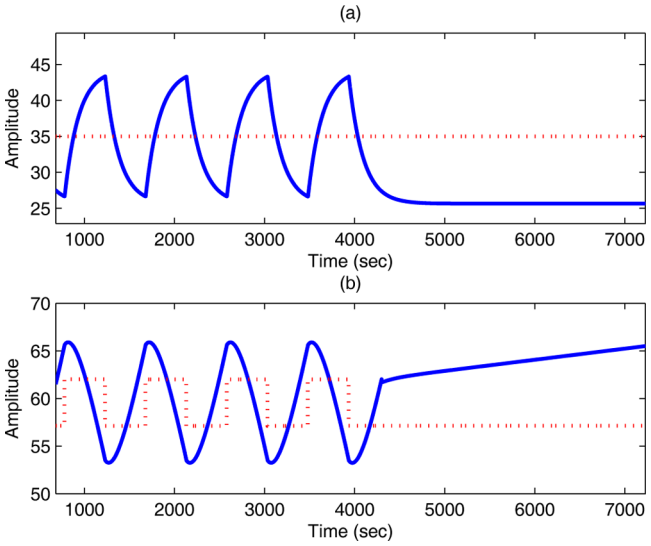

Figure 20. Signals in example 4: (a) $y_m(t)$ (solid) and $r(t)$ (dash), (b) $m(t)$ (solid) and $v(t)$ (dash).

5. CONCLUSION

This paper proposed a closed-loop compensation method to remove the oscillations caused by control valve stiction. The proposed method added a short-time rectangular wave to the reference to enable the control valve to arrive at the desired position with two movements. The parameters of the short-time rectangular wave were designed in a systematic manner. The steps of the proposed closed-loop compensation method were given at the flowchart in Figure 6. Some laboratory and simulations examples illustrated the effectiveness of the proposed method.

The proposed method was presented for the FOPDT process model in eq 2 and the PI controller in eq 3. As known from the design procedure, it is feasible to generalize the proposed method for more general process models and controllers. Besides the stiction model[17] adopted here, there are other data-driven stiction models available in literature. The design principle of the proposed method can be followed to design new compensation methods for these stiction models.

As a future work, a theoretical analysis needs to be performed to study the effect of the uncertainties of the estimated parameters on the compensation method. The difficulty for such a theoretical analysis lies at the complex relationship between the design parameters and estimated parameters in eqs 26 and 42, the lower bounds of r_c in eqs 30 and 36, and the upper bounds of r_c in eqs 32, 34, 35 and 40. Another future work is to integrate the proposed compensation method with an online oscillation method such as the one in our recent study[28] to detect the reappearance of oscillations and to initiate the compensation steps in an automatic manner. That is, once the oscillation is detected online, the required parameters of the process and stiction models can be re-estimated if necessary, and the proposed compensation method with the updated design parameters can be implemented again to remove the oscillation.

AUTHOR INFORMATION

Corresponding Author

*To whom correspondence should be addressed E-mail: jiandong@pku.edu.cn. Phone: +86(10)6275-3856. Fax: +86(10)6275-7426.

Notes

The authors declare no competing financial interest.

■ ACKNOWLEDGMENTS

The author thanks the National Natural Science Foundation of China for financial grants No. 61074105 and No. 61061130559.

■ REFERENCES

(1) Bialkowski, W. Dreams versus reality: a view from both sides of the gap. *Pulp Pap. Can.* **1993**, *94*, 19−27.
(2) Desborough, L.; Nordh, P.; Miller, R. Control system reliability: process out of control. *Ind. Comput.* **2001**, *8*, 52−55.
(3) Paulonis, M.; Cox, J. A practical approach for large-scale controller performance assessment, diagnosis, and improvementl. *J. Process Control* **2003**, *13*, 155−168.
(4) Jelali, M.; Huang, B. *Detection and Diagnosis of Stiction in Control Loops: State of the Art and Advanced Methods*; Springer Verlag, 2010.
(5) Gerry, J.; Ruel, M. How to measure and combat valve stiction online. *2011 ISA Technical Conference*, Houston, TX, September, **2001**.
(6) Choudhury, M.; Shah, S.; Thornhill, N. Modeling valve stiction. *Control Eng. Pract.* **2005**, *13*, 641−658.
(7) Hägglund, T. A friction compensation for pneumatic control valves. *J. Process Control* **2002**, *12*, 897−904.
(8) Hägglund, T. Automatic on-line estimation of backlash in control loops. *J. Process Control* **2007**, *17*, 489−499.
(9) Srinivasan, R.; Rengaswamy, R. Stiction compensation in process control loops: A framework for integrating stiction measure and compensation. *Ind. Eng. Chem. Res.* **2005**, *44*, 9164−9174.
(10) Ivan, L.; Lakshminarayanan, S. A new unified approach to valve stiction quantification and compensation. *Ind. Eng. Chem. Res.* **2009**, *48*, 3474−3483.
(11) Srinivasan, R.; Rengaswamy, R. Approaches for efficient stiction compensation in process control valves. *Comput. Chem. Eng.* **2008**, *32*, 218−229.
(12) Cuadros, M.; Munaro, C.; Munareto, S. Improved stiction compensation in pneumatic control valves. *Comput. Chem. Eng.* **2012**, *38*, 106−114.
(13) Cuadros, M.; Munaro, C.; Munareto, S. Novel model-free approach for stiction compensation in control valves. *Ind. Eng. Chem. Res.* **2012**, *51*, 8465−8476.
(14) Mohammad, M.; Huang, B. Compensation of control valve stiction through controller tuning. *J. Process Control* **2012**, *22*, 1800−1819.
(15) Armstrong-Hélouvry, B.; Dupont, P.; de Wit, C. A survey of models, analysis tools and compensation methods for the control of mechines with friction. *J. Process Control* **1994**, *30*, 1083−1138.
(16) Kayihan, A.; Doyle, F. Friction compensation for a process control valve. *Control Eng. Pract.* **2000**, *8*, 799−812.
(17) He, Q.; Wang, J.; Pottmann, M.; Qin, S. A curve fitting method for detecting valve stiction in oscillating control loops. *Ind. Eng. Chem. Res.* **2007**, *46*, 4549−4560.
(18) Seborg, D.; Edgar, T.; Mellichamp, D. *Process Dynamics and Control*, 2nd ed.; John Wiley & Sons: Hoboken, NJ, 2004.
(19) Srinivasan, R.; Rengaswamy, R.; Narasimhan, S.; Miller, R. Control loop performance assessment. 2. Hammerstein model approach for stiction diagnosis. *Ind. Eng. Chem. Res.* **2004**, *44*, 6719−6728.
(20) Jelali, M. Estimation of valve stiction in control loops using separable least squares and global search algorithms. *J. Process Control* **2008**, *18*, 632−642.
(21) Choudhury, M.; Jain, M.; Shah, S. Stiction—definition, modeling, detection and quantification. *J. Process Control* **2008**, *18*, 232−243.
(22) Karra, S.; Karim, M. Comprehensive methodology for detection and diagnosis of oscillatory control loops. *Control Eng. Pract.* **2009**, *17*, 939−956.
(23) Farenzena, M.; Trierweiler, J. Valve stiction estimation using global optimization. *Control Eng. Pract.* **2012**, *20*, 379−385.
(24) Ljung, L. *System Identification: Theory for the User*, 2nd ed.; Prentice Hal: Englewood Cliffs, N.J., 1999.
(25) Zhu, Y. *Multivariable System Identification for Process Control*; Elsevier Science: Oxford, 2001.
(26) Tjarnstrom, F.; Ljung, L. Variance properties of a two-step ARX estimation procedure. *Eur. J. Control* **2003**, *9*, 422−430.
(27) Ljung, L.; Wills, A. Issues in sampling and estimating continuous-time models with stochastic disturbances. *Automatica* **2010**, *46*, 925−931.
(28) Wang, J.; Huang, B.; Lu, S. Improved DCT-based method for online detection of oscillations in univariate time series. *Control Eng. Pract.* **2013**, *21*, 622−630.